



Suppression of ferromagnetism in La_3CrAs_5 via V substitution

Lei Duan^a, Yanteng Wei^a, Hanlu Zhang^a, Xiancheng Wang^{b,c,*}, Suxuan Du^a, Yagang Feng^a, Shichang Cai^a, Jianfa Zhao^b, Jun Zhang^b, Zhe Wang^{d,*}, Changqing Jin^{b,c,e,*}

^a School of Materials Science and Engineering, Henan University of Technology, Zhengzhou 450007, China

^b Beijing National Laboratory for Condensed Matter Physics, Institute of Physics, Chinese Academy of Sciences, Beijing 100190, China

^c School of Physics, University of Chinese Academy of Sciences, Beijing 100190, China

^d College of Chemistry and Material Science, Hebei Normal University, Shijiazhuang 050024, China

^e Materials Research Lab at Songshan Lake, Dongguan 523808, China

ARTICLE INFO

Keywords:

Ferromagnetic order
Chemical substitution
Metal
Spin glass

ABSTRACT

In this work, we successfully synthesized a series of hexagonal $\text{La}_3\text{Cr}_{1-x}\text{V}_x\text{As}_5$ ($x = 0-0.8$) polycrystalline samples under high-temperature and high-pressure conditions. A systematic study was carried out via the measurements of X-ray powder diffraction, temperature- and field-dependent magnetic susceptibility and magnetization. The X-ray diffraction data show that the lattice constant a -parameter gradually increases, while c -parameter decreases with increasing V-doping level. In this series, the ferromagnetic behavior has been observed for $x \leq 0.3$, and the Curie temperature T_C decreases from 50 K for the parent compound to 20 K for $x = 0.3$, which indicates that the ferromagnetism is suppressed as the V-doped increases. For $x = 0.4$, the system begins to enter into a new magnetic state like spin glass at low temperature, and no magnetic order can be observed down to 2 K for $x \geq 0.8$. In addition, the Weiss temperature T_θ gradually decreases and changes to be negative for $x = 0.6$, which suggests that ferromagnetic interaction at first is weakened by the V substitution, and then transforms into anti-magnetic predominant interaction. The above results indicate that there is no quantum criticality occurred in the $\text{La}_3\text{Cr}_{1-x}\text{V}_x\text{As}_5$ system.

1. Introduction

A quantum critical point (QCP) occurs when a material undergoes a continuous transition from one state to another at the absolute zero temperature, which is driven by quantum fluctuation, instead of thermal fluctuation [1,2]. At the vicinity of QCP, a plenty of exotic physical properties can be generated, such as non-Fermi liquid behavior [3,4], even unconventional superconductivity [5,6], spin resonances [7] and so on. In general, it is a very fruitful way to search a QCP by suppressing a magnetic phase transition to zero temperature by a tuning parameter, such as, pressure, chemical substitutions and magnetic field [8]. There are a lot of experimental evidences that many anti-ferromagnetic systems can be tuned to a QCP, such as $(\text{Ce}_{1-x}\text{Y}_x)_2\text{Ir}_3\text{Ge}_5$ [9], TiSe_2 [10] and $\text{EuCu}_2(\text{Ge}_{1-x}\text{Si}_x)_2$ [11]. However, ferromagnetic QCP is much less known both from the theoretical and experimental points of view [12]. Therefore, it is of special interest to investigate ferromagnetic metals where the ferromagnetic transition temperature T_C can be driven to 0 K by tuning external parameters.

LaCrGe_3 has been reported to crystallize in a hexagonal structure with space group $P6_3/mmc$. The structure contains face-sharing octahedral CrAs_6 chains along c -axis, which are arranged triangularly in the ab -plane [13]. It is reported that LaCrGe_3 is a ferromagnetic metal with $T_C \sim 78$ K. To suppress the ferromagnetism in $\text{LaV}_x\text{Cr}_{1-x}\text{Ge}_3$ system, the substitution of V for Cr has been studied and the results show the magnetic exchange interactions are changed and the long-range ferromagnetic order is suppressed with the V substitution [14]. Besides the chemical substitution, the external pressure was also applied on LaCrGe_3 . Although the ferromagnetic phase was suppressed near 2.1 GPa, quantum criticality is avoided by the appearance of a new magnetic phase [15,16]. However, a wing structure phase diagram leading towards quantum wing critical point at high field occurs as the application of magnetic field [17]. Recently, we have reported a new quasi-one-dimensional compound La_3CrAs_5 synthesized under the high pressure and high temperature conditions [18]. Similar to LaCrGe_3 , the structure of La_3CrAs_5 consists of face-sharing CrAs_6 chains, packed in a triangular lattice in ab -plane, as shown in Fig. 1(a) and (b). However, for La_3CrAs_5 ,

* Corresponding authors.

E-mail addresses: wangxiancheng@iphy.ac.cn (X. Wang), wangzhe@hebtu.edu.cn (Z. Wang), jin@iphy.ac.cn (C. Jin).

<https://doi.org/10.1016/j.jmmm.2023.171583>

Received 19 September 2023; Received in revised form 15 November 2023; Accepted 28 November 2023

Available online 1 December 2023

0304-8853/© 2023 Elsevier B.V. All rights reserved.

the CrAs₆ chains are separated by two octahedral AsLa₆ chains. Thus the distance of adjacent chains is significantly enlarged from 6.195 Å for LaCrGe₃ to 8.984 Å for La₃CrAs₅. More importantly, physical properties show that La₃CrAs₅ also is a metal and undergoes a ferromagnetic order with $T_c \sim 50$ K, which is similar to that of LaCrGe₃ [18,19]. Therefore, the substitution of V for Cr in La₃Cr_{1-x}V_xAs₅ offers a possibility to suppress the ferromagnetic order of La₃CrAs₅ and search a QCP in this system like LaCrGe₃.

In this paper, we report the synthesis of polycrystalline La₃Cr_{1-x}V_xAs₅ ($x = 0-0.8$) samples and a systematic study on their structure and magnetic properties. The ferromagnetic ordering is suppressed with the V concentration increasing, and the system enters into a new magnetic ground state, possibly a spin glass state for x up to 0.4. For even higher V-doped compounds $x \geq 0.8$, no magnetic order can be observed down to 2 K. No quantum critical point can be approached in the La₃Cr_{1-x}V_xAs₅ system.

2. Experimental

A series of polycrystalline samples La₃Cr_{1-x}V_xAs₅ ($x = 0, 0.1, 0.3, 0.4, 0.6, 0.8$) were synthesized under the high pressure and high temperature conditions. The experimental details have been reported in Ref [18]. The X-ray diffraction measurements were carried out on a Rigaku Ultima VI (3 KW) diffractometer using Cu K α radiation ($\lambda = 1.54060$ Å) generated at 40 kV and 40 mA with a scanning rate of 1°/min and a scanning step length of 0.02°. Rietveld refinements on the diffraction patterns were performed using GSAS software packages. Magnetic measurements were performed using a superconducting quantum interference device (SQUID). The temperature dependence of the magnetic susceptibility was measured in the temperature range of 2–300 K under the field of 0.1 T. Isothermal magnetization curves were measured at 2 K with the magnetic field varying from -7 T to 7 T.

3. Results and discussion

Fig. 2 shows the Rietveld refinement of room temperature powder X-ray diffraction pattern of La₃Cr_{1-x}V_xAs₅ ($x = 0, 0.1, 0.3, 0.4, 0.6, 0.8$). It is observed that all these diffraction pattern can be indexed into a hexagonal structure with the space group $P6_3/mcm$ (No. 193). Here, the structure of La₃CrAs₅ with the space group $P6_3/mcm$ was adopted as the initial model to carry out the refinement for the XRD data. The crystallographic data were obtained and summarized in Table 1. In the case of undoped La₃CrAs₅, the obtained lattice parameters are $a = 8.9889(1)$ Å and $c = 5.8927(8)$ Å, agreed with the previously reported values [18]. The doping dependence of lattice parameters (a and c) and cell volumes (V) are shown in Fig. 3. One can see that a , c and V monotonically change as the x increases, which indicates that the Cr atoms in La₃CrAs₅ are properly replaced by V atoms.

Owing to the smaller ionic radius of V, the lattice parameters of the La₃Cr_{1-x}V_xAs₅ system should gradually decrease as the doped V increases. However, the a -parameter gradually increases, while c -

parameter decreases, which has been observed in similar LaV_xCr_{1-x}Ge₃ system [14]. We speculate that these results may derive from the decrease of the angles $\angle\text{As-Cr-As}$ (α) in the CrAs₆ octahedron, as shown in Fig. 1(b), which indicates that the La₃Cr_{1-x}V_xAs₅ samples are compressed along the c axis, but stretched along the ab plane as the V-doped content increases.

The dc magnetic susceptibility measurement for La₃Cr_{1-x}V_xAs₅ samples was carried out with an applied field of 0.1 T in both zero-field-cooled (ZFC) and field-cooled (FC) modes, as shown in Fig. 4. For $x = 0$, the parent compound La₃CrAs₅, the magnetic susceptibility curves display a rapid increase near 50 K and tend to be saturated as the temperature decreases, suggesting a paramagnetic-ferromagnetic transition. The similar temperature-dependent of susceptibility for the same compound was reported in literature [18]. In addition, it is observed that with increasing V concentration x until $x \leq 0.3$, all the susceptibility curves increase suddenly at some temperature and tend to saturate at low temperature like the parent compound, which indicates that these doped samples also display a ferromagnetic behavior. In order to confirm the ferromagnetic transition temperature for $x \leq 0.3$, the temperature derivative of magnetic susceptibility is presented in the Fig. S1 (see the Supplementary Materials). The peak corresponding to the ferromagnetic transition can be clearly observed, and T_c is determined and also shown in the Fig. S1. It is seen that the ferromagnetic transition temperature T_c decreases from 50.4 K in La₃CrAs₅ down to 11.6 K in La₃Cr_{0.3}V_{0.7}As₅, suggesting that the V-doped suppresses the ferromagnetism of the parent compound La₃CrAs₅. Simultaneously, the magnitude of the magnetization gradually decreases for $x \leq 0.3$. However, when the doping V concentration x increases to 0.4, the magnitude of the magnetization, which is about ten times smaller than that of doped sample for $x = 0.3$, rapidly decreases. The inset of Fig. 4 shows that the enlarged view of magnetic susceptibility for $x \geq 0.4$ in the range temperature of 2–20 K. It is noted that the ZFC and FC curves are overlapped at high temperature region but slightly split at lower temperature with $x = 0.4$ and 0.6, which is different from these samples for $x \leq 0.3$ and indicates a spin glass ground state. Furthermore, for $x = 0.8$, there is no bifurcation down to 2 K (see the inset of Fig. 4), and the ZFC and FC curves are overlapped in the whole measured temperature and demonstrate paramagnetic-like behavior.

In order to further study the magnetism of the doped sample for $x \geq 0.4$, we measured the susceptibility curves for La₃Cr_{0.6}V_{0.4}As₅ sample with applied different field of 0.005 T – 0.1 T. The enlarged view in the temperature range of 2–20 K is shown in Fig. 5. The ZFC and FC curves begin to bifurcate and demonstrate a λ -shape, and the intensity of the ZFC/FC curves is suppressed with increasing magnetic field, which is different from the ferromagnetic materials where the intensity of the susceptibility curve increases as the magnetic field increases. It is possible that with the continuous suppression of ferromagnetism, the magnetic behavior in this series evolves from a ferromagnetic state into a new magnetic state. In addition, as shown in Fig. 5, there is a local maximum T_f , which can be observed in the FC curve, and the T_f decreases gradually as the applied field increases. The above results are

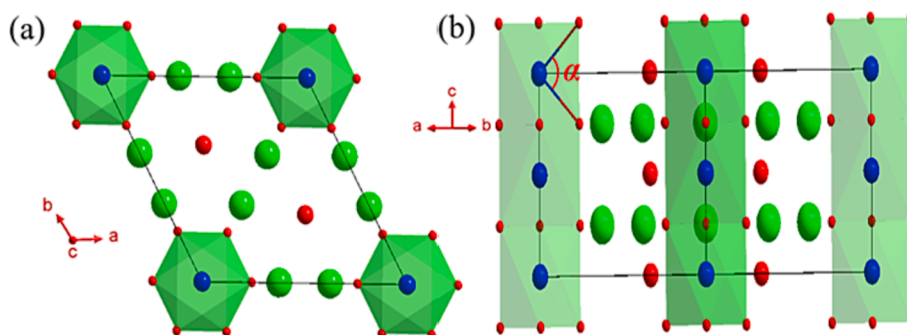


Fig. 1. (a) and (b) shows the crystal structures of La₃CrAs₅. Green represents the La cation, Blue denotes the Cr cation, and Red represents the Ge or As ions.

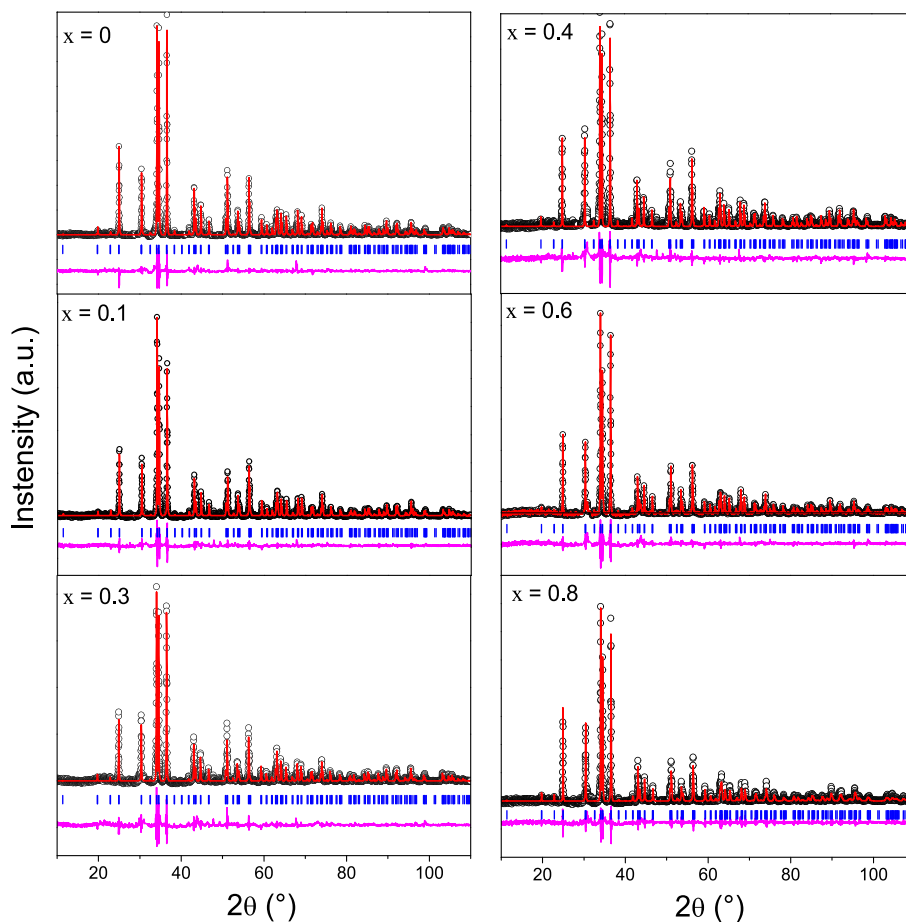


Fig. 2. The powder X-ray diffraction patterns of $\text{La}_3\text{Cr}_{1-x}\text{V}_x\text{As}_5$ ($x = 0, 0.1, 0.3, 0.4, 0.6, 0.8$) and the refinement with the space group of $P6_3/mcm$ (No. 193).

typical characteristics for a spin glass system, which indicates that the magnetic state possibly transforms from a ferromagnetic state to a spin glass state with increasing V concentration x .

The inverse susceptibility as the function of temperature for $\text{La}_3\text{Cr}_{1-x}\text{V}_x\text{As}_5$ ($x = 0-0.8$) is plotted in Fig. 6. In the high temperature region, the curves of all the compounds display linear-like behavior, which can be described by the Curie-Weiss law $1/\chi = (T - T_\theta)/C$, where C is the Curie constant and T_θ is the Weiss temperature. By fitting the magnetic susceptibility within the temperature range of 150–300 K with the Curie-Weiss law, we can obtain the Curie constant C and the Weiss temperature T_θ , as shown in Table 2. Using the formula $\mu_{\text{eff}} = \sqrt{8C}$, the effective moment μ_{eff} per molecule was calculated and also listed in Table 1. For $x = 0$, μ_{eff} is found to be about $3.06 \mu_{\text{B}}/\text{f.u.}$, which is consistent with the reported value [18]. With increasing V concentration, μ_{eff} gradually decreases but does not approach zero even as x reaches 0.8 (shown in Table 2). In addition, it is observed that the Curie-Weiss temperature T_θ gradually decreases from 91.3 K in parent compound La_3CrAs_5 to 9.6 K in $\text{La}_3\text{Cr}_{0.6}\text{V}_{0.4}\text{As}_5$. However, when $x = 0.6$, the Curie-Weiss temperature T_θ turns to be negative (-6.0 K). These results indicate that in the series of $\text{La}_3\text{Cr}_{1-x}\text{V}_x\text{As}_5$, ferromagnetic interaction at first is weakened by the V substitution, and then transforms into anti-ferromagnetic predominant interaction for $x \geq 0.6$.

To further understand the nature of magnetism of the $\text{La}_3\text{Cr}_{1-x}\text{V}_x\text{As}_5$ ($x = 0, 0.1, 0.3, 0.4, 0.6, 0.8$) samples, we performed the measurement of isothermal dependences of magnetization at 2 K. For the doped samples with $x \leq 0.3$, the magnetization tends to saturate, suggesting the existence of ferromagnetic interaction in these compounds. Moreover, the saturate moment μ_s gradually decreases from $1.81 \mu_{\text{B}}/\text{f.u.}$ for parent compound to $0.92 \mu_{\text{B}}/\text{f.u.}$ for $\text{La}_3\text{Cr}_{0.7}\text{V}_{0.3}\text{As}_5$, as shown in Fig. 7

(a), which indicates that the ferromagnetic interaction is weakened as the doped V content increases. Fig. 7(b) displays the isothermal dependences of magnetization of the doped samples with $x \geq 0.4$. It can be observed that “S-shape” curves occur at 2 K, but it does not reach saturation even the magnetic field up to 7 T, which indicates the $\text{La}_3\text{Cr}_{1-x}\text{V}_x\text{As}_5$ series for $x \geq 0.4$ is no longer ferromagnetic. The result is a common phenomenon in the spin glass system [20,21], which is consistent with the susceptibility curves and then confirms the spin glass state for $x \geq 0.4$.

The ferromagnetism in the $\text{La}_3\text{Cr}_{1-x}\text{V}_x\text{As}_5$ series has been able to be suppressed via chemical substitution. A phase diagram of transition temperature T_c/T_f as a function of V-doped content x for $\text{La}_3\text{V}_x\text{Cr}_{1-x}\text{As}_5$ is plotted in Fig. 8. As we can see, there are three potential types of the low temperature magnetic behavior in the $\text{La}_3\text{Cr}_{1-x}\text{V}_x\text{As}_5$ series. The first one is a ferromagnetic phase for x up to 0.3. The ferromagnetic transition temperature T_c is obtained by the temperature derivative of magnetic susceptibility (as shown in Fig. S1). It is gradually suppressed by V doping from 50.4 K for $x = 0$ down to 11.6 K for $x = 0.3$. For $x = 0.4$ and 0.6, the magnetic susceptibility curves both exhibit a “ λ ” shape behavior. It seems that there is a transition from the ferromagnetic state to a spin glass-like state. The transition temperature T_f is determined by the local maximum observed in the FC curve. When x increases to 0.8, no magnetic order can be observed down to 2 K, which indicates that there are two possibilities of magnetic properties for $x \geq 0.8$. One is that the T_f of spin glass behavior is lower than 2 K. The other one is that the magnetic behavior may enter into a new complex magnetic state. Further investigations are needed to determine the exact concentration at which the transition occurs.

Fig. 9(a) shows the estimated Curie-Weiss temperature T_θ and the effective moment μ_{eff} per molecule as a function of V-doped content x .

Table 1Crystallographic data for $\text{La}_3\text{Cr}_{1-x}\text{V}_x\text{As}_5$ ($x = 0, 0.1, 0.3, 0.4, 0.6, 0.8$).

Hexagonal structure; Space group: $P6_3/mcm$, No. 193						
La_3CrAs_5 $\text{La}_3\text{Cr}_{0.9}\text{V}_{0.1}\text{As}_5$ $\text{La}_3\text{Cr}_{0.7}\text{V}_{0.3}\text{As}_5$ $\text{La}_3\text{Cr}_{0.6}\text{V}_{0.4}\text{As}_5$ $\text{La}_3\text{Cr}_{0.4}\text{V}_{0.6}\text{As}_5$						
$\text{La}_3\text{Cr}_{0.2}\text{V}_{0.8}\text{As}_5$						
$a = 8.9889(2) \text{ \AA}$ $a = 8.9903(1) \text{ \AA}$ $a = 8.9918(2) \text{ \AA}$ $a = 8.9942(2) \text{ \AA}$ $a = 8.9959(5) \text{ \AA}$						
$a = 8.9979(1) \text{ \AA}$						
$c = 5.8927(1) \text{ \AA}$ $c = 5.8907(1) \text{ \AA}$ $c = 5.8874(3) \text{ \AA}$ $c = 5.8834(1) \text{ \AA}$ $c = 5.8834(2) \text{ \AA}$						
$c = 5.8755(3) \text{ \AA}$						
$\chi^2 = 2.72$; $R_p = 3.4\%$ $\chi^2 = 1.92$; $R_p = 2.6\%$ $\chi^2 = 3.10$; $R_p = 4.5\%$ $\chi^2 = 2.69$; $R_p = 3.7\%$ $\chi^2 = 2.91$; $R_p = 3.1\%$ $\chi^2 = 1.78$; $R_p = 2.1\%$						
$R_{wp} = 4.1\%$ $R_{wp} = 3.3\%$ $R_{wp} = 5.9\%$ $R_{wp} = 5.6\%$ $R_{wp} = 4.9\%$ $R_{wp} = 2.7\%$						
site	Wyck	x	y	z	Occ.	$100 \times U (\text{\AA}^2)$
La_3CrAs_5						
La	6g	0.6229(2)	0	0.25	1	0.0099(2)
Cr	2b	0	0	0	1	0.0269(3)
As1	6g	0.2465(7)	0	0.25	1	0.0159(2)
As2	4d	1/3	2/3	0	1	0.0257(6)
$\text{La}_3\text{Cr}_{0.9}\text{V}_{0.1}\text{As}_5$						
La	6g	0.6247(1)	0	0.25	1	0.0097(1)
Cr	2b	0	0	0	0.9	0.0051(3)
V	2b	0	0	0	0.1	0.0051(3)
As1	6g	0.2455(1)	0	0.25	1	0.0038(5)
As2	4d	1/3	2/3	0	1	0.0257(1)
$\text{La}_3\text{Cr}_{0.7}\text{V}_{0.3}\text{As}_5$						
La	6g	0.6188(4)	0	0.25	1	0.0102(3)
Cr	2b	0	0	0	0.7	0.0268(3)
V	2b	0	0	0	0.3	0.0268(3)
As1	6g	0.2437(1)	0	0.25	1	0.0008(4)
As2	4d	1/3	2/3	0	1	0.0341(2)
$\text{La}_3\text{Cr}_{0.6}\text{V}_{0.4}\text{As}_5$						
La	6g	0.6234(1)	0	0.25	1	0.0063(5)
Cr	2b	0	0	0	0.6	0.0264(3)
V	2b	0	0	0	0.4	0.0264(3)
As1	6g	0.2423(2)	0	0.25	1	0.0039(4)
As2	4d	1/3	2/3	0	1	0.0300(1)
$\text{La}_3\text{Cr}_{0.4}\text{V}_{0.6}\text{As}_5$						
La	6g	0.6212(1)	0	0.25	1	0.0109(1)
Cr	2b	0	0	0	0.4	0.0241(7)
V	2b	0	0	0	0.6	0.0241(7)
As1	6g	0.2413(1)	0	0.25	1	0.0029(4)
As2	4d	1/3	2/3	0	1	0.0274(5)
$\text{La}_3\text{Cr}_{0.2}\text{V}_{0.8}\text{As}_5$						
La	6g	0.6212(1)	0	0.25	1	0.0119(3)
Cr	2b	0	0	0	0.2	0.0179(2)
V	2b	0	0	0	0.8	0.0179(2)
As1	6g	0.2413(1)	0	0.25	1	0.0008(1)
As2	4d	1/3	2/3	0	1	0.0273(3)

As x increases, T_θ decreases monotonically from 91.3 K to -32.4 K, which suggests that the ferromagnetic interaction is suppressed and turns to be anti-ferromagnetic. The effective moment μ_{eff} per molecule also decreases with the increasing x . It is worth noting that when supposed that the V ions have no contribution on the effective moment μ_{eff} , we can calculate and obtain effective moment $\mu_{\text{eff}}/\text{Cr}$. However, it is found that the effective moment $\mu_{\text{eff}}/\text{Cr}$ increases as the x increases, which is opposite to that of the $\text{LaCr}_{1-x}\text{V}_x\text{Ge}_3$ system [14]. In addition, the effective moment $\mu_{\text{eff}}/\text{Cr}$ is found to be $8.35 \mu_B/\text{Cr}$ for $x = 0.8$, which is obviously unreasonable. The above results indicate that the contribution of V ions on the effective moment μ_{eff} cannot be ignored, and then may influences the magnetic exchange interaction in the $\text{La}_3\text{Cr}_{1-x}\text{V}_x\text{As}_5$ system. Furthermore, the saturated moments μ_s per molecule of the $\text{La}_3\text{Cr}_{1-x}\text{V}_x\text{As}_5$ series were plotted in Fig. 9(b). For higher V doped compounds ($x \geq 0.4$), the $\text{La}_3\text{Cr}_{1-x}\text{V}_x\text{As}_5$ system is no longer ferromagnetic. Hence, the $\mu_s/\text{f. u.}$ is replaced by the value of magnetization at 7 T.

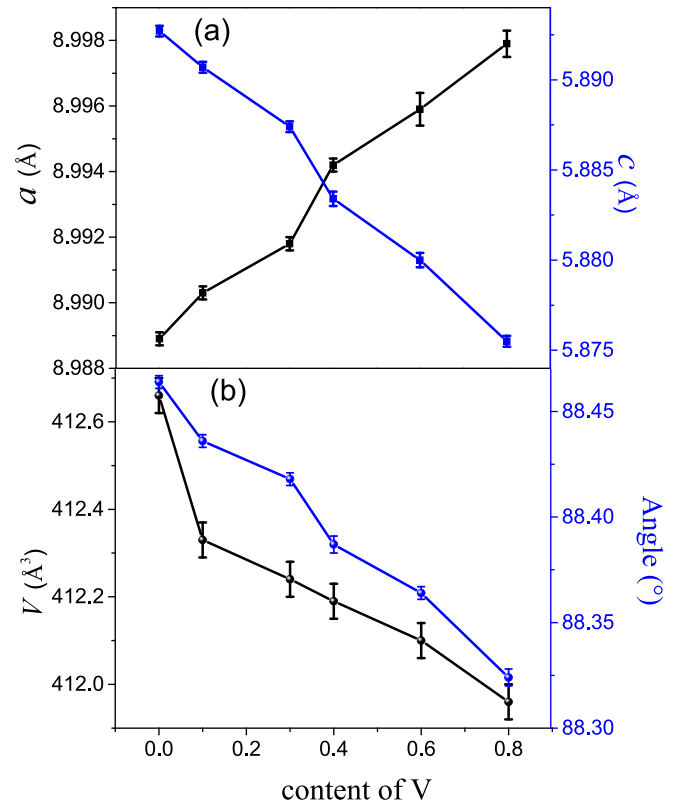


Fig. 3. (a) show the lattice parameters a and c of $\text{La}_3\text{Cr}_{1-x}\text{V}_x\text{As}_5$ samples as a function of V concentration. (b) the variation of the cell volumes and angles of $\angle\text{As-Cr-As}$ in CrAs_6 octahedron of $\text{La}_3\text{Cr}_{1-x}\text{V}_x\text{As}_5$ samples.

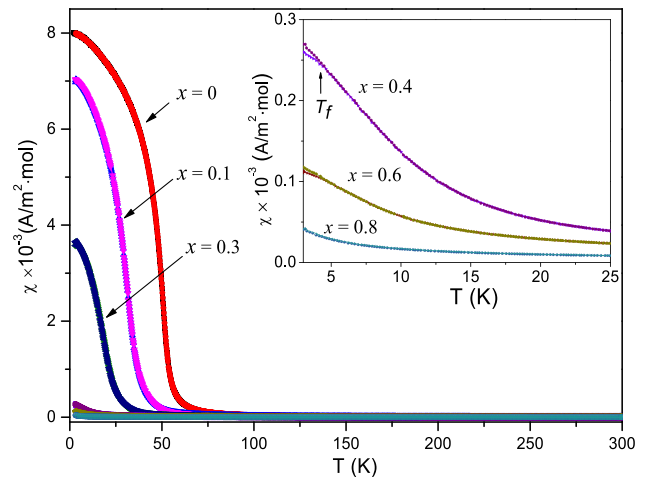


Fig. 4. The magnetic susceptibility as a function of temperature under ZFC and FC conditions for $\text{La}_3\text{Cr}_{1-x}\text{V}_x\text{As}_5$ ($x = 0, 0.1, 0.3, 0.4, 0.6, 0.8$) samples. The inset shows the low temperature parts for $x = 0.4, 0.6, 0.8$.

It is seen that the $\mu_s/\text{f. u.}$ for $x = 0.8$ (only $\sim 0.14 \mu_B$) is very small compared with the parent compound, which indicates that the contribution of V on saturated moments μ_s can be ignored in comparison with Cr ions. Hence, μ_s/Cr can be calculated and also plotted in Fig. 9(b). As the V-doped content x increases, μ_s/Cr gradually decreases, similar to that of the $\text{LaCr}_{1-x}\text{V}_x\text{Ge}_3$ system [14].

For the parent compound La_3CrAs_5 , the estimated effective moment μ_{eff} ($\sim 3.06 \mu_B$) and saturation moment μ_s ($\sim 1.81 \mu_B$) both are smaller than the expected values for a localized spin-only moment for high-spin Cr^{3+} ion, which indicates the existence of itinerant ferromagnetism in

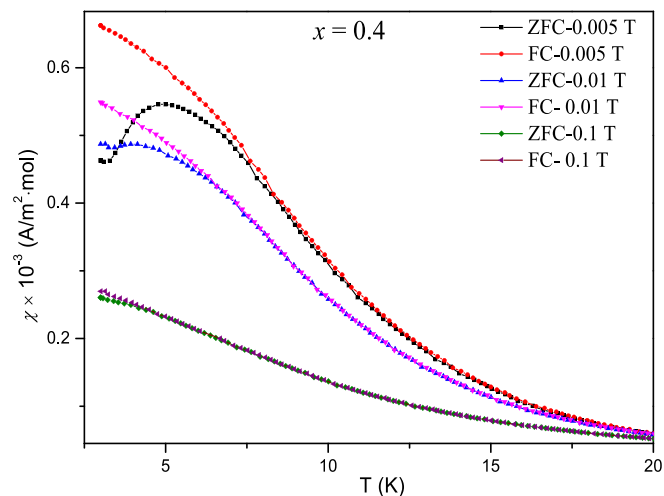


Fig. 5. Temperature dependent of dc susceptibility curves for the $\text{La}_3\text{Cr}_{0.6}\text{V}_{0.4}\text{As}_5$ sample under various magnetic field of 0.005 T – 0.1 T.

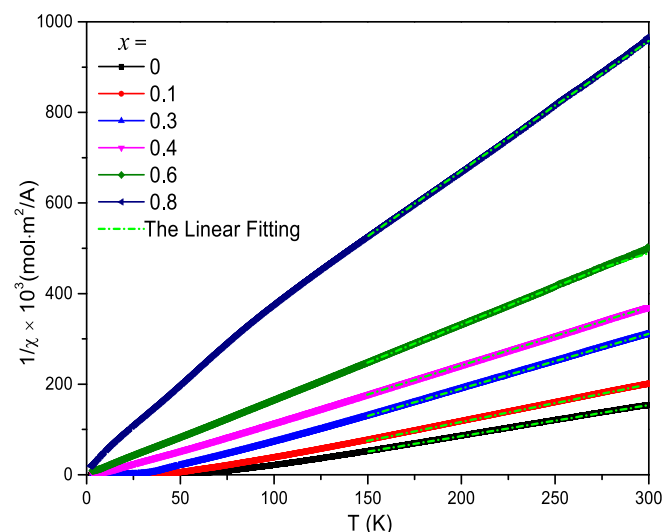


Fig. 6. Temperature dependence of inverse susceptibility for $\text{La}_3\text{Cr}_{1-x}\text{V}_x\text{As}_5$ samples ($x = 0, 0.1, 0.3, 0.4, 0.6, 0.8$).

Table 2

Summarized transition temperatures, Curie-Weiss temperature T_θ , effective moment μ_{eff} , saturated moment μ_s .

x	T_c (T_f) (K)	T_θ (K)	μ_{eff} ($\mu_B/\text{f.u.}$)	μ_s ($\mu_B/\text{f.u.}$)
0	50.4	91.3	3.06	1.81
0.1	31.5	65.0	2.98	1.47
0.3	11.6	52.7	2.44	0.91
0.4	4.6	9.6	2.14	–
0.6	3.5	–6.0	1.96	–
0.8	–	–32.4	1.67	–

La_3CrAs_5 , similar to LaCrGe_3 . When substituting V for Cr in $\text{La}_3\text{V}_x\text{Cr}_{1-x}\text{Ge}_5$ system, the estimated effective moment μ_{eff} and saturated moments μ_s per Cr decrease as the V concentration increases, which indicates that the system possesses a fragile ferromagnetism and it may be a potential QCP system [14]. However, although the magnetism in the doped $\text{La}_3\text{V}_x\text{Cr}_{1-x}\text{As}_5$ system also is can be easily perturbed, the doped V ions possibly influence the magnetic interaction, which is contrasted to that of $\text{La}_3\text{V}_x\text{Cr}_{1-x}\text{Ge}_5$ system [14], and causes non-negligible contribution on the effective moment μ_{eff} . Furthermore, the

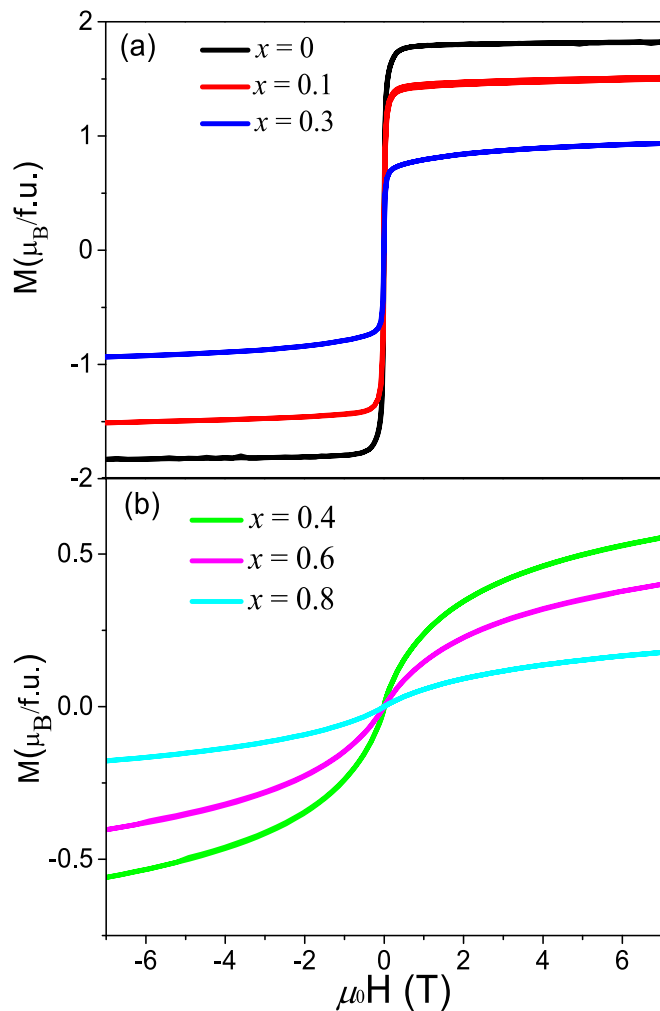


Fig. 7. The magnetic hysteresis curves measured at 2 K for $\text{La}_3\text{Cr}_{1-x}\text{V}_x\text{As}_5$ samples, (a) for $x = 0, 0.1, 0.3$; (b) for $x = 0.4, 0.6, 0.8$.

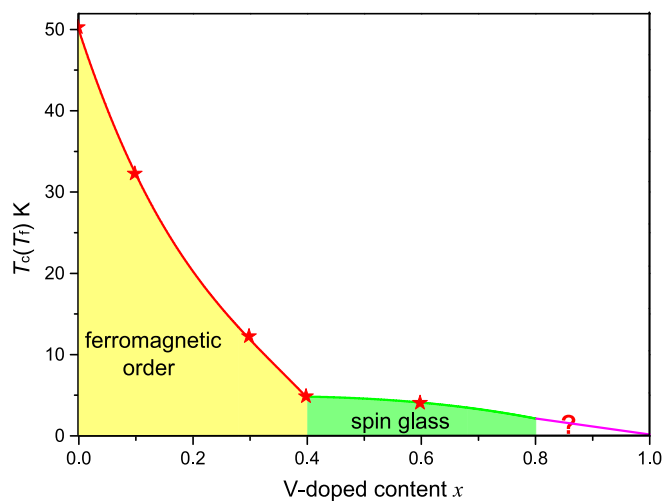


Fig. 8. Magnetic phase diagram of $\text{La}_3\text{Cr}_{1-x}\text{V}_x\text{As}_5$.

$(\text{Cr}/\text{V})\text{As}_6$ chains are arranged in a triangular lattice in the ab -plane, which generally causes the magnetic frustration, like La_3CrAs_5 and La_3MnAs_5 compounds [18,22]. As we know, magnetic frustration usually can lead to the spin glass state [21] and reduced ordered moment

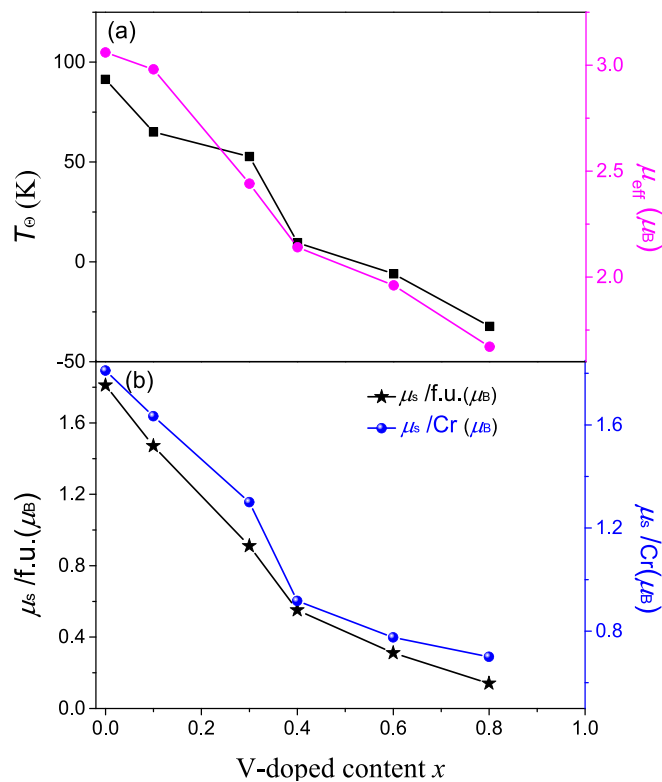


Fig. 9. (a) the estimated Curie-Weiss temperature T_0 and the effective moment μ_{eff} per molecule as a function of x ; (b) the saturated moments μ_s /f.u. and μ_s /Cr as a function of the V-doped content x .

[23]. Hence, it is speculated that the magnetic contribution of V ions and magnetic frustration may result in a reduction of saturation moment and play an important role in the formation of complex magnetic behavior in the $\text{La}_3\text{Cr}_{1-x}\text{V}_x\text{As}_5$ system.

4. Conclusions

In summary, a series of $\text{La}_3\text{Cr}_{1-x}\text{V}_x\text{As}_5$ ($x = 0-0.8$) compounds have been synthesized under high-temperature and high-pressure conditions, and systemic measurements on their structure and magnetic properties were carried out. As the V-doped content increases, the ferromagnetism in this series is gradually suppressed, and then involves into a new ground magnetic state like spin glass for $x = 0.4$. Furthermore, no long-range magnetic order can be observed above 2 K for $x = 0.8$. The quantum criticality is avoided by the formation of spin glass-like magnetic ground state, which is considered to possibly result from the magnetic contribution of V ions and magnetic frustration.

CRedit authorship contribution statement

Lei Duan: Formal analysis, Investigation, Data curation, Writing – original draft, Writing – review & editing, Visualization. **Yanteng Wei:** Formal analysis, Data curation, Writing – original draft, Visualization. **Hanlu Zhang:** Data curation, Visualization. **Xiancheng Wang:** Conceptualization, Formal analysis, Writing – original draft, Writing – review & editing. **Suxuan Du:** Data curation, Visualization. **Yagang Feng:** Data curation, Visualization. **Shichang Cai:** Formal analysis, Writing – original draft. **Jianfa Zhao:** Formal analysis, Supervision. **Jun Zhang:** Formal analysis, Writing – review & editing. **Zhe Wang:** Formal analysis, Writing – original draft, Writing – review & editing. **Changqing Jin:** Conceptualization, Project administration, Formal analysis, Writing – original draft, Resources.

Declaration of competing interest

The authors declare that they have no known competing financial interests or personal relationships that could have appeared to influence the work reported in this paper.

Data availability

Data will be made available on request.

Acknowledgments

We greatly appreciate the support of the Doctoral Fund of Henan University of Technology under Grant No. 2020BS029, China Postdoctoral Science Foundation under Grant Nos. 2023M741036, the National Key R&D Program of China under Grant No. 2023YFA1406000 and Hebei Natural Science Foundation under Grant Nos. B202020504. This research is also supported by the Key Scientific and Technological Research Projects in Henan Province under Grant No. 222102240091 and Natural Science Foundation from the Department of Science & Technology of Henan Province under Grant No. 232300420309.

Appendix A. Supplementary data

Supplementary data to this article can be found online at <https://doi.org/10.1016/j.jmmm.2023.171583>.

References

- [1] J.A. Hertz, Quantum critical phenomena, *Phys. Rev. B* 14 (1976) 1165–1184.
- [2] S. Sachdev, Theory of finite-temperature crossovers near quantum critical points close to, or above, their upper-critical dimension, *Phys. Rev. B* 55 (1997) 142.
- [3] C. Pfeiderer, S.R. Julian, G.G. Lonzarich, Non-Fermi-liquid nature of the normal state of itinerant-electron ferromagnets, *Nature* 414 (2001) 22.
- [4] W.K. Huang, S. Hosoi, M. Culo, S. Kasahara, Y. Sato, K. Matsuura, Y. Mizukami, M. Berben, N.E. Hussey, H. Kontani, T. Shibauchi, Y. Matsuda, Non-Fermi liquid transport in the vicinity of the nematic quantum critical point of superconducting $\text{FeSe}_{1-x}\text{S}_x$, *Phys. Rev. R* 2 (2020), 033367.
- [5] C. Pfeiderer, M. Uhlarz, S.M. Hayden, R. Vollmer, H.v. Loëhneysen, N.R. Bernhoeft, G.G. Lonzarich, Coexistence of superconductivity and ferromagnetism in the d-bandmetal ZrZn_2 , *Letters to, Nature* 412 (2001) 5.
- [6] C.Z. Wang, S. Liu, H. Jeon, Y. Jia, J. Cho, Charge density wave and superconductivity in the kagome metal CsV_3Sb_5 around a pressure-induced quantum critical point, *Phys. Rev. M* 6 (2022), 094801.
- [7] E.M. Bittar, C. Adriano, C. Giles, C. Rettori, Z. Fisk, P.G. Pagliuso, Probing the localized to itinerant behavior of the 4f electron in $\text{CeIn}_{3-x}\text{Sn}_x$ by Gd^{3+} electron spin resonance, *Phys. Rev. B* 86 (2012), 125108.
- [8] M. Brando, D. Belitz, F.M. Grosche, T.R. Kirkpatrick, Metallic quantum ferromagnets, *Rev. Modern Phys.* 88 (2016), 025006.
- [9] R. Khan, K. Althubeiti, M. Algethami, N. Rahman, M. Sohail, Q. Mao, Q. Zaman, A. Ullah, N. Ilyas, A. Mohammad Afzal, A. Khan, M. Akif Safeen, A. Khan, Observation of quantum criticality in antiferromagnetic based $(\text{Ce}_{1-x}\text{Y}_x)_2\text{Ir}_3\text{Ge}_5$ Kondo-Lattice system, *J. Magn. Magn. Mater.* 556 (2022), 169361.
- [10] S. Lee, T.B. Park, J. Kim, S.-G. Jung, W.K. Seong, N. Hur, Y. Luo, D.Y. Kim, T. Park, Tuning the charge density wave quantum critical point and the appearance of superconductivity in TiSe_2 , *Phys. Rev. R* 3 (2021), 033097.
- [11] M.A. Ahmida, M. Forthaus, C. Geibel, Z. Hossain, G.R. Hearne, J. Kaštil, J. Prchal, V. Sechovský, M.M. Abd-Elmeguid, Charge fluctuations across the pressure-induced quantum phase transition in $\text{EuCu}_2(\text{Ge}_{1-x}\text{Six})_2$, *Phys. Rev. B* 101 (2020), 205127.
- [12] H. Kotegawa, E. Matsuoka, T. Uga, M. Takemura, M. Manago, N. Chikuchi, H. Sugawara, H. Tou, H. Harima, Indication of Ferromagnetic Quantum Critical Point in Kondo Lattice CeRh_5Ge_4 , *J. Phys. Soc. Japan* 88 (2019), 093702.
- [13] H. Bie, O. Ya, A.V. Tkachuk, A. Mar, Structures and Physical Properties of Rare-Earth Chromium Germanides RECrGe_3 ($\text{RE} = \text{La}-\text{Nd}, \text{Sm}$), *Chem. Mater.* 18 (2007) 4613–4620.
- [14] X. Lin, V. Taufour, S.L. Bud'ko, P.C. Canfield, Suppression of ferromagnetism in the $\text{LaV}_x\text{Cr}_{1-x}\text{Ge}_3$ system, *Phys. Rev. B* 88 (2013), 094405.
- [15] E. Gati, J.M. Wilde, R. Khasanov, L. Xiang, S. Dissanayake, R. Gupta, M. Matsuda, F. Ye, B. Haberl, U. Kaluarachchi, R.J. McQueeney, A. Kreyssig, S.L. Bud'ko, P. C. Canfield, Formation of short-range magnetic order and avoided ferromagnetic quantum criticality in pressurized LaCrGe_3 , *Phys. Rev. B* 103 (2021), 075111.
- [16] V. Taufour, U.S. Kaluarachchi, R. Khasanov, M.C. Nguyen, Z. Guguchia, P. K. Biswas, P. Bonfa, R. De Renzi, X. Lin, S.K. Kim, E.D. Mun, H. Kim, Y. Furukawa, C.Z. Wang, K.M. Ho, S.L. Bud'ko, P.C. Canfield, Ferromagnetic quantum critical point avoided by the appearance of another magnetic phase in LaCrGe_3 under pressure, *Phys. Rev. Lett* 117 (2016), 037207.

- [17] U.S. Kaluarachchi, S.L. Bud'ko, P.C. Canfield, V. Taufour, Tricritical wings and modulated magnetic phases in LaCrGe_3 under pressure, *Nat. Commun.* 8 (2017) 546.
- [18] L. Duan, X. Wang, F. Zhan, J. Zhang, Z. Hu, J. Zhao, W. Li, L. Cao, Z. Deng, R. Yu, H.-J. Lin, C.-T. Chen, R. Wang, C. Jin, High-pressure synthesis, crystal structure and physical properties of a new Cr-based arsenide La_3CrAs_5 , *Sci. China Mater.* 63 (2020) 1750–1758.
- [19] L. Duan, X. Wang, J. Zhang, J. Zhao, Z. Zhao, C. Xiao, C. Guan, S. Wang, L. Shi, J. Zhu, C. Jin, Critical behavior of the ferromagnetic metal La_3CrAs_5 with quasi-one-dimensional spin chains, *J. Alloys. Compds.* 905 (2022), 164214.
- [20] L. Duan, X. Wang, J. Zhao, J. Zhang, S. Du, Y. Feng, Z. Zhao, S. Wang, C. Jin, High-pressure synthesis and physical properties of a spinel compound FeAl_2S_4 , *Inorg. Chem.* 61 (2022) 13184–13190.
- [21] L. Duan, X.-C. Wang, J. Zhang, J.-F. Zhao, L.-P. Cao, W.-M. Li, R.-Z. Yu, Z. Deng, C.-Q. Jin, Synthesis, structure, and properties of $\text{Ba}_9\text{Co}_3\text{Se}_{15}$ with one-dimensional spin chains, *Chin. Phys. B* 29 (2020), 036102.
- [22] L. Duan, X.C. Wang, J. Zhang, Z. Hu, J.F. Zhao, Y.G. Feng, H.L. Zhang, H.J. Lin, C. T. Chen, W. Wu, Z. Li, R. Wang, J.F. Zhang, T. Xiang, C.Q. Jin, Synthesis, structure, and magnetism in the ferromagnet La_3MnAs_5 : Well-separated spin chains coupled via itinerant electrons, *Phys. Rev. B* 106 (2022), 184405.
- [23] E. Lhotel, S. Petit, S. Guitteny, O. Florea, M. Ciomaga Hatnean, C. Colin, E. Ressouche, M.R. Lees, G. Balakrishnan, Fluctuations and all-in-all-out ordering in dipole-octupole $\text{Nd}_2\text{Zr}_2\text{O}_7$, *Phys. Rev. Lett.* 115 (2015), 197202.